energies

MDPI

Article

Impact of Biofuel Blending on Hydrocarbon Speciation and Particulate Matter from a Medium-Duty Multimode Combustion Strategy

Yensil Park, Melanie Moses-DeBusk *, Scott S. Sluder and Shean P. Huff

Oak Ridge National Laboratory, Oak Ridge, TN 37831, USA; parky@ornl.gov (Y.P.); sluders@ornl.gov (S.S.S.); huffsp@ornl.gov (S.P.H.)

* Correspondence: mosesmj@ornl.gov

Abstract: The U.S. Department of Energy's Co-Optima initiative simultaneous focused on diversifying fuel sources, improving efficiency, and reducing emissions through using novel combustion strategies and sustainable fuel blends. For medium-duty/heavy-duty diesel engines, research in this area has led to the development of a multimode strategy that uses premixed charge compression ignition (PCCI) at low loads and conventional diesel combustion (CDC) at mid–high loads. The aim of this study was to understand how emissions were impacted when using PCCI instead of CDC at low loads and switching to an oxygenated biofuel blend. It provides a detailed speciation of the hydrocarbon (HC) and particulate matter (PM) emissions from a multimode medium-duty engine operating at low loads in PCCI and CDC modes and high loads in CDC. The effect of the oxygenated biofuel blend on emissions was studied at all three mode–load conditions using #2 ULSD and a bio-derived fuel (25% hexyl hexanoate (HHN)) blended in #2 ULSD. The PCCI mode effectively decreased NOx, total HC, and PM/PN emissions, with a substantial decrease in larger particles (≥50 nm). A PM/PN reduction was observed at high loads with the 25% HHN fuel. While the total HC emissions were not impacted by fuel type, the detailed HC analysis exposed changes in the HC's composition.

Keywords: multimode; medium duty; PCCI; biofuel; emissions; particulate matter; hydrocarbons

Citation: Park, Y.; Moses-DeBusk, M.; Sluder, S.S.; Huff, S.P. Impact of Biofuel Blending on Hydrocarbon Speciation and Particulate Matter from a Medium-Duty Multimode Combustion Strategy. *Energies* **2023**, *16*, 5735. https://doi.org/10.3390/en16155735

Academic Editor: Vladislav A. Sadykov

Received: 2 June 2023
Revised: 21 June 2023
Accepted: 22 June 2023
Published: 1 August 2023

1. Introduction

In response to climate change concerns, the United States government is targeting a 50–52% net greenhouse gas reduction by 2030, reaching net-zero emissions by 2050 [1]. To achieve these goals in the transportation sector, an eclectic range of technologies will be required, including carbon-free and low-carbon fuels such as electricity, hydrogen, and biofuels. The sectors that pose challenges for electrification, such as those requiring medium-duty and heavy-duty (MDHD) engines, require efforts to enhance efficiency and reduce emissions while ensuring feasible costs and practicality in real-world operations. Continuous improvements in hybridization and advanced combustion strategies are viable solutions to achieve these goals of improving efficiency and lowering emissions. The MDHD vehicle sector covers a wide range of drive cycles, from stop-and-go routes of local delivery trucks and public buses to long-haul freight trucks. These varying MDHD drive cycles also differ from light-duty vehicles. For example, class 8 trucks consume about 18–25 times more fuel and cover 5.5 times greater mileage annually than light-duty vehicles [2]. MDHD vehicles are a critical market that can reduce greenhouse gas (GHG) emissions through hybridization; however, this requires battery and infrastructure advancements [3,4]. The wide variety of MDHD vehicles, including in their weight, size, and drive cycle, complicates these infrastructure solutions.

Low-temperature combustion (LTC) strategies maintain high engine efficiency while decreasing engine emissions, making them promising combustion solutions in an eclectic portfolio for reducing GHGs. Significant LTC advancements have been made over the last

two decades, but extending the operational range to high loads has been a major challenge. Homogeneous charge compression ignition (HCCI) combustion has been well documented in the literature to significantly lower engine emissions while maintaining high thermal efficiency [5,6], but controlling its combustion phasing is difficult due to the impact of chemical kinetics on combustion timing. Premixed charge compression ignition (PCCI) combustion is another way to achieve LTC that provides better control of combustion than HCCI, making it a bridge between CDC and HCCI combustions [7,8].

The final phase of the U.S. Department of Energy's (DOE) Co-Optimization of Fuels and Engines (Co-Optima) initiative focused on an integrated approach to improve MDHD efficiency and push towards net-zero carbon emissions. The initiative first focused on a collaborative effort to screen multiple potential fuel blendstocks that could be bio-derived to address net-zero carbon issues, maintained good diesel-range fuel properties for mixing controlled compression-ignition (MCCI or CDC), and could meet production and operational cost requirements [9]. A Co-Optima engine study confirmed the use of the blendstocks for CDC combustion [10]. Another study developed low-load PCCI strategies with two of the down-selected oxygenated blendstocks, hexyl hexanoate (HHN) and dibutoxymethane, in an MD single-cylinder diesel engine, and the findings revealed that PCCI conditions can further lower NOx and filter smoke number emissions without increasing HC emissions [11]. Bio-derived HHN, which can be formed from the esterification of hexanoic acid with 1-hexyl alcohol, has a straight-chain structure with an ester group in the middle of the molecule. HHN has a cetane number similar to typical ultra-low sulfur diesel (ULSD) market fuel and was selected for this study.

A multimode engine operates in two or more different combustion modes by switching between LTC and CDC modes to efficiently reduce emissions across different operational ranges. Combining PCCI and CDC into a multimode strategy can help overcome the operation range limitations common to LTC strategies like PCCI. This study examined the impact of using the bio-blendstock fuel, 25 vol% HHN, in #2 ULSD in comparison to neat #2 ULSD, on emissions from a PCCI-CDC multimode engine. This MDHD multimode strategy uses PCCI combustion at low-load and CDC at high-load operation. This deep-dive emission study investigated the fuel and mode impact on the detailed HC speciation and the particulate matter (PM) emissions.

2. Materials and Methods

2.1. Engine Setup and Operation

The engine used in this study was a single-cylinder MD diesel engine modified from a 6.7 L Cummins, 6-cylinder ISB engine by deactivating 5 cylinders. The engine geometric specifications are described in Table 1. The same engine was also used in a previously reported study focused on the multimode engine operation strategy which contains more engine configuration details [11,12]. The engine was operated under standard CDC or PCCI modes at 1.8 bar (low load) or 3.2 bar (high load) at constant speed (1200 rpm).

Table 1. Engine specifications.

Displacement (L)	1.12
Bore (mm)	107
Stroke (mm)	124
Connecting Rod (mm)	145.4
Compression Ratio	20:1
Fuel Injector	CRIN-3, 8-hole, 145° included angle

2.2. Fuels

Both emissions certification #2 ULSD and a 25 vol% blend of HHN in #2 ULSD fuels were used in this study. The blend fuel was mixed in-house by splash blending and analyzed by Southwest Research Institute. Results are described in Table 2. There are two oxygen atoms per HHN molecule, so blending 25 vol% of HHN into #2 ULSD added 4.24 wt% oxygen to the fuel. The cetane numbers of #2 ULSD and the HHN-blended fuel are similar.

Table 2. Properties of #2 ULSD and 25 vol% HHN in #2 ULSD fuel blend at atmospheric pressure.

	#2 ULSD	25 vol% HHN in #2 ULSD
Cetane Number	46.9	45.7
Carbon Content (wt%)	86.24	82.64
Hydrogen Content (wt%)	13.44	13.12
Oxygen Content (wt%)	N/A	4.24
Net Heat of Combustion(MJ/kg)	43.09	41.2
Density@ 15 °C (g/mL)	0.8455	0.8490
T50 (°C)	275	248.9
T90 (°C)	341	335.0
FBP (°C)	361	356.7

2.3. Emission Sampling

Gaseous and PM emission sampling and analysis were performed with multiple different techniques. Direct sampling ports were used to sample exhaust gas for Fourier-transform infrared spectroscopy (FTIR), Micro Soot Sensor (MSS), and Engine Exhaust Particle Sizer (EEPS) measurements. A fourth sampling port pulled exhaust flow into a custom dilution sampling tunnel. The basic layout of the dilution tunnel is shown in Figure 1 and was based on previous studies [13]. Briefly, an orifice and ejector pump combo were used to pull exhaust flow into the tunnel, where it was diluted by triple-filtered dry air controlled by a Teledyne mass flow controller (MFC). The dilution ratio of the dilution tunnel was controlled by the orifice and air flow rate and kept between 8 and 9 for all the experimental conditions. Physical PM samples were collected on filters for both total gravimetric mass and elemental and organic carbon (EC/OC) mass speciation. Samples for off-line speciation of small gaseous hydrocarbons and aldehydes were also taken from this dilution tunnel. The temperature of the sampling tunnel was kept at 47 °C during sampling.

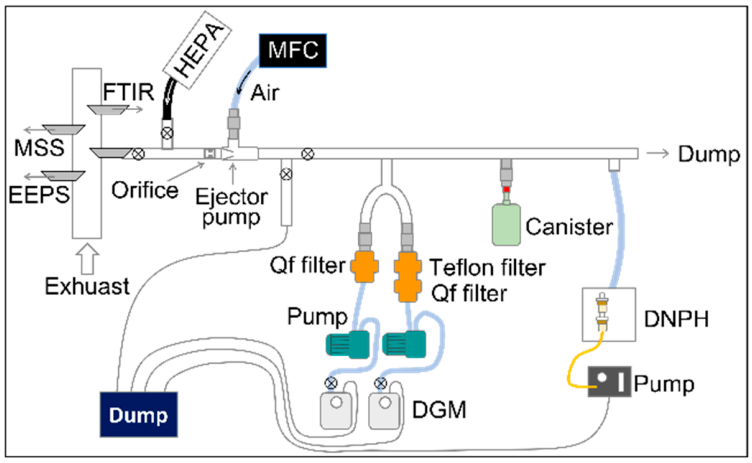

Figure 1. Schematic picture of the dilution tunnel setup for emissions sample collection.

2.3.1. Gaseous Emissions

Standard engine exhaust measurements were taken with a standard 5-gas emissions bench using instruments purchased from California Analytical Instruments (CAI). The sampling lines from the exhaust were kept at 191 °C to prevent condensation. Total unburned hydrocarbons (THCs) were measured on a C1 basis by the CAI flame ionization detector (FID). Other gases analyzed by the standard emissions bench included CO, CO_2, NO, and NO_2. More detailed gaseous emissions were sampled by FTIR and from the custom dilution tunnel for off-line analysis.

FTIR

A fast MKS 5 Hz FTIR sampled the exhaust directly without dilution. A diaphragm pump was used to pull the sampled exhaust through a heated filter before entering the FTIR. Heated lines were used to maintain the sampled exhaust at 191 °C. MKS FTIR

software methods provided predefined list of HC species for gasoline and diesel engine exhaust analysis. Consecutive measurements were taken at conditions studied using gasoline (g-FTIR) and diesel (d-FTIR) methods. The MKS g-FTIR method used in this study included 15 different HC species, while the d-FTIR method included only 8 different HC species. Consistent FTIR results were seen for species contained in both methods. The "diesel C1" measurement in the d-FTIR method, which was developed by MKS through a calibration using vaporized #2 ULSD fuel, was correlated in this study to THC FID analyzer readings. In the Results and Discussion sections, the THCs from FID results are compared to that from both g-FTIR and d-FTIR results, where g-FTIR is the sum of all 15 HC species and d-FTIR is only the "diesel C1" value.

Canister (GC-MS)

Volatile HC samples were collected from the custom dilution tunnel with cleaned pre-evacuated MiniCan™ canisters from Entech Instruments (Simi Valley, CA, USA) and analyzed off-line by GC-MS from Agilent Technologies (Santa Clara, CA, USA). Measured HCs reported in this study are grouped by their functionality, such as paraffins, olefins, and aromatics. Accurate quantification of high-boiling-point, semi-volatile HC species is difficult using this technique due to lower response factors. Therefore, the quantification was only measured and reported for relatively low carbon numbers (aromatics: $C \leq 9$, paraffins/olefins: $C \leq 10$).

DNPH (HPLC-UV/Vis)

Dilute exhaust samples were pulled at 1 L/min from the custom dilution tunnel for 20 min through Sep-Pak DNPH (2,4-dinitrophenylhydrazine) cartridges by Waters Corporation (Milford, MA, USA). The complexed aldehydes trapped by the DNPH were removed from the solid-phase extraction cartridge with 3 mL of acetonitrile then analyzed using HPLC-UV/vis. Two DNPH cartridges in series were used for each condition to ensure correct measurements in the event that an oversaturation of the front cartridge occurred.

2.3.2. PM/PN Emissions

MSS

Soot emissions were sampled directly from the exhaust by an AVL Micro Soot Sensor (MSS) using an AVL heated sample line and internally diluted by the MSS conditioning system. All data reported have been dilution-corrected and converted to a soot mass rate using the total exhaust flow rate.

Particle Samplings

EC/OC and gravimetric samples were collected from the custom dilution tunnel on pre-fired quartz fiber (Qf) and pre-weighed 47 mm $PM_{2.5}$ PTFE filters, respectively. The dilute exhaust was pulled through a single sampling port on the tunnel then split in a y-configuration into two parallel sample streams using separate pumps and dry gas meters (DGM). One diluted sample stream was pulled through a single filter holder loaded with a Qf filter. The other sample stream was pulled through an in-series double sample holder loaded with the second Qf behind a PTFE filter. The collected particle samples on Qfs were sent to Sunset Laboratory, Inc. to measure EC/OC mass loading by NIOSH method [14] for each condition. The PM samples collected on PTFE filters were weighed in-house for total gravimetric PM mass measurement.

EEPS

Exhaust particle number (PN) rate and size distributions were measured with a TSI Engine Exhaust Particle Sizer (EEPS; TSI model 3090). Exhaust samples were pulled from the exhaust through a heated (191 °C) line into a custom-made double-dilution tunnel that has been previously reported [13]. Briefly, the double-dilution tunnel consisted of two stages separated by a thermal evaporator section. Each dilution stage used triple-filtered air and an orifice and an ejector pump setup to dilute the exhaust. The hot exhaust was diluted with 150 °C dilution

air before entering and passing through the evaporator section, which heated the dilute exhaust to 350 °C to evaporate semi-volatiles that may have condensed on the particles. After thermal denuding of the particles at 350 °C, the dilute exhaust was diluted a second time and allowed to cool to 50 °C before being sampled by the EEPS. Data were collected for 120 s at each condition once the engine was stable, then averaged and converted from a volumetric concentration into a rate (#/min) for comparison between different engine mode conditions.

3. Results

The naming convention and load–mode matrix studied are shown in Table 3. Fuel-mode comparisons between PCCI and CDC1 were performed at the low-load condition, while the fuel–load impact was compared using CDC modes; low load (CDC1) and high load (CDC2) were compared at the same speed.

Table 3. Naming and matrix of conditions studied.

	HHN	#2 ULSD
Low Load (1.8 bar)	PCCI	PCCI
Low Load (1.8 bar)	CDC1	CDC1
High Load (3.2 bar)	CDC2	CDC2

3.1. Gaseous Emissions

3.1.1. Criteria Emissions

Figure 2 summarizes gaseous emissions from PCCI, CDC1, and CDC2 modes with two different fuels, #2 ULSD and 25% HHN blended in #2 ULSD, in a MD multimode engine. The PCCI strategy significantly reduced NOx emissions and THCs; however, the lower THC mass rate of PCCI came at the expense of increased CO emissions. Using HHN blend fuel slightly increased CO and THC emissions in the PCCI mode, but the criteria emissions trends were the same regardless of fuel types. The consistency in CO_2 emissions between PCCI and CDC1 suggests a similar degree of combustion efficiency.

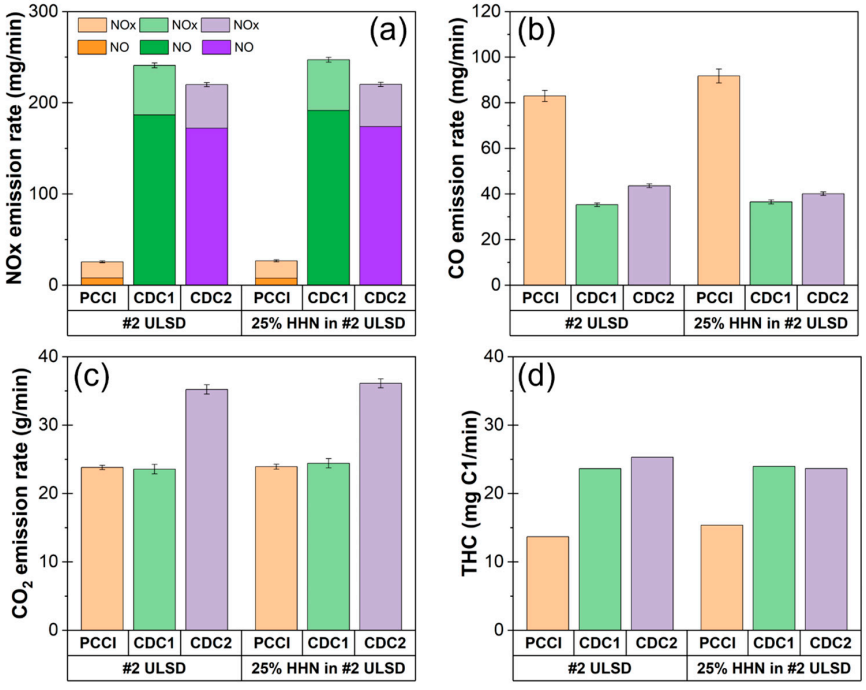

Figure 2. (**a**) NOx, (**b**) CO, (**c**) CO_2 emissions measured with FTIR, and (**d**) THC emissions measured with FID from ACI and two different loads in CDC modes with #2 ULSD and HHN blended fuel in the medium-duty, multimode engine.

3.1.2. HC Emission Speciation

THC engine emissions are traditionally measured by FID analyzers designed to measure HC concentrations reported on a C1 basis. While this is the standard method for evaluating and comparing THC emissions between engine exhaust studies, it fails to accurately measure oxygenated HCs and provides no speciation details. Speciated THC emission data can indicate different reaction pathways or be used to tailor emissions to control catalyst solutions. FTIR analysis can deliver real-time speciation of the HC exhaust components, as well as standard criteria pollutants. As the number of carbons in the HC species increases, it becomes more difficult for an in-line FTIR to distinguish and quantify them due to an overlap of C–H stretching frequencies between similar species [15]. Recent reports, however, have shown FTIR to be effective at delivering a good representation of the functional distribution of HC emissions from gasoline-range combustion strategies [16,17]. Since this MDHD multimode study used diesel-range fuels, a standard diesel FTIR (d-FTIR) method was used for the analysis. The d-FTIR method identified some small HCs, but only a single aldehyde (formaldehyde), and lumped all large HCs into a single "Diesel C1" concentration, failing to provide the level of speciation seen in the studies with gasoline-range fuels. Therefore, a second FTIR measurement was also performed at each condition using a gasoline FTIR (g-FTIR) method. Figure 3 compares the FID THC mass rate results to both the d-FTIR and g-FTIR results, and all results are presented as C1 mass rates. The g-FTIR stacked-plot data show the functional distribution of the HCs.

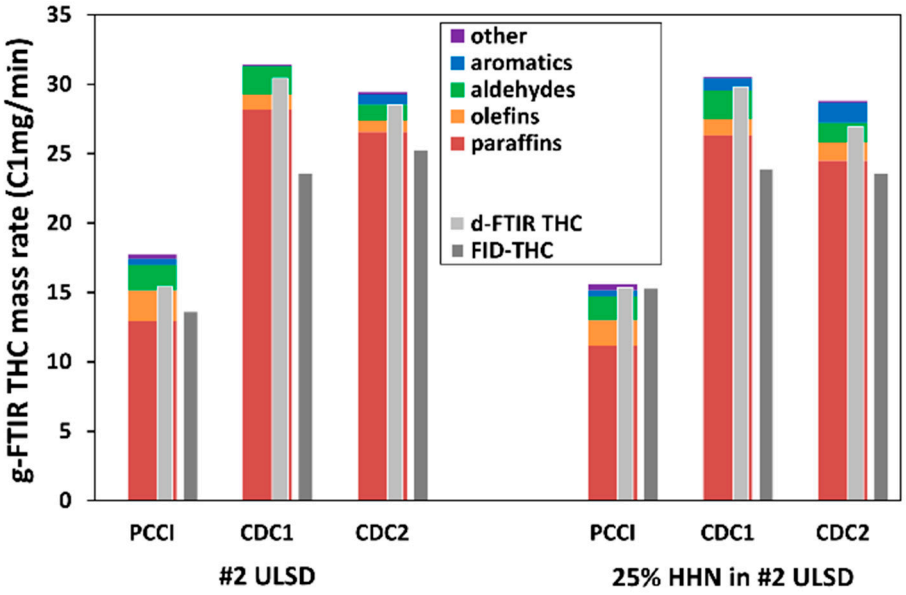

Figure 3. HC results from FTIR spectra taken with gasoline method (g-FTIR, speciated stacked bars), diesel method (d-FTIR, light gray), and FID-THC (dark gray).

There was good agreement between the total C1 mass rates from the g-FTIR and d-FTIR, but these were slightly higher than the C1 mass rate measured by FID. The THCs from g-FTIR were slightly higher than d-FTIR in all conditions, but the results from the two FTIR methods agreed reasonably well with each other. The FID, which has a poor oxygenate response, showed 10–22% lower THC results than FTIR except in the PCCI mode with 25% HHN fuel. Although the d-FTIR method does not account for all the aldehydes, the FID does not account for any formaldehyde and then underestimates the C1 mass for all larger aldehydes. The d-FTIR included smaller C2–C4 hydrocarbons but was devoid of partial fuel combustion products that fall in the C5–C12 range. The g-FTIR filled this gap in speciation and was therefore used to provide the functional distribution of the HC emissions. Considering that limitations exist for each of these analytical techniques, which

prevent accurate measurement of the large mix of unknown hydrocarbons present in engine exhaust, the similarities between them suggest they provide a useful first approximation.

The amount of THCs in PCCI exhaust was reduced by 45–65%, depending on the measurement methods, compared to CDC1 for both fuels. The g-FTIR results in Figure 3 show that this reduction was predominantly associated with paraffins, while slight olefin increases were observed for both #2 ULSD and 25% HHN fuels. Comparing CDC1 and CDC2, small decreases in THCs were detected by both FTIR methods when load increased, whereas a slight increase or no change was indicated by the FID measurement. g-FTIR measurements indicate that paraffins and aldehydes were the two main HC species that decreased from CDC1 to CDC2 as aromatics increased. Using 25% HHN fuel shows a slight decrease in THCs without any notable fraction changes in PCCI mode but increased aromatic HC emissions in CDC modes.

More detailed aldehyde speciation, collected with DNPH cartridges, was converted to the C1 mass rates shown in Figure 4 and compared with the total aldehyde mass rate measured by g-FTIR. The C1 aldehyde rate trends from two different methods were in good agreement. There were eleven different aldehyde species detected with the DNPH method, but the two major species in all conditions were formaldehyde and acetaldehyde.

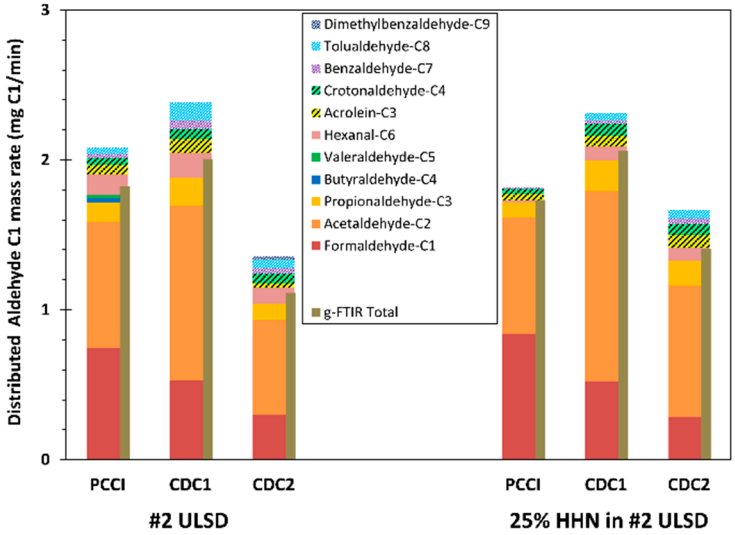

Figure 4. Total aldehyde C1 mass rates direct from g-FTIR (thin gold bar) compared to C1 mass species distributions derived from DNPH analysis (stacked bars).

Comparing the two low-load modes, the PCCI mode reduced the total aldehyde emissions, predominately associated with a drop in paraffinic and aromatic aldehydes for both fuels. Despite the overall aldehyde C1 emission drop, a notable increase in formaldehyde emissions occurred in the PCCI mode regardless of fuel type. While CDC2 operation produced lower aldehyde emissions for both fuels compared to either low-load condition, the drop was not as significant for the oxygenated 25% HHN fuel. However, PCCI mode with the oxygenated 25% HHN fuel resulted in lower aldehyde emissions, most notably through the elimination of the large C4-C6 paraffinic and aromatic aldehydes.

The detailed speciation of the larger and non-oxygenated HCs sampled with canisters and analyzed by GC-MS is shown grouped by functionality in Figure 5. FTIR is a powerful tool for HC speciation, but is more effective at measuring smaller HC molecules, as discussed earlier. The canister data included a wide variety of HC species from C3 to C14; however, we combined the quantified larger volatile paraffins and olefins $\leq$ C10 and aromatics $\leq$ C9 due to a limitation of the technique being that it cannot accurately quantify bigger molecules. The total amount of quantifiable HC from canister sampling, for each of the three conditions, was less than half of the C1 seen by FID.

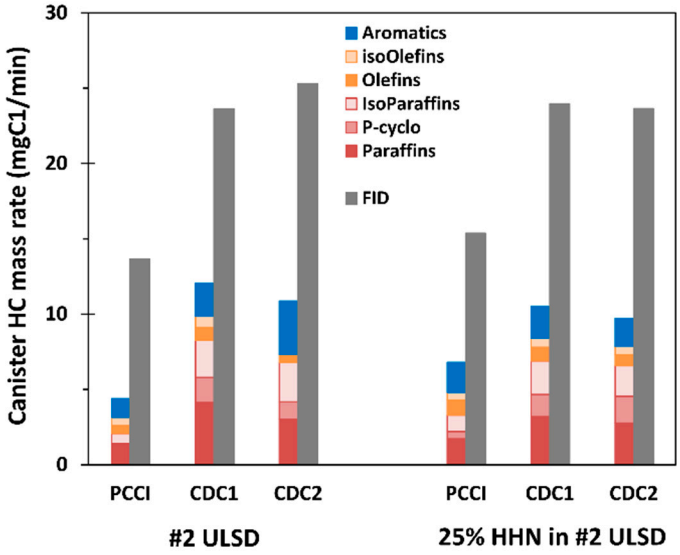

Figure 5. Grouped HC species analyzed from canister samples compared with FID data.

3.2. Particulate Matter Emissions

The effects of biofuel from a multimode engine on PM emissions are summarized in Figure 6. PM contains elemental carbon (EC), soot PM, and organic carbon (OC). Three different methods were used to measure PM mass rate including gravimetrical measurements (similar to the EPA regulatory process) and a thermal optical method which quantified the PM carbon mass contribution from both EC and OC, following the NIOSH method [14]. The standard soot mass was measured by an AVL MSS and correlates with the EC PM measured by the NIOSH method.

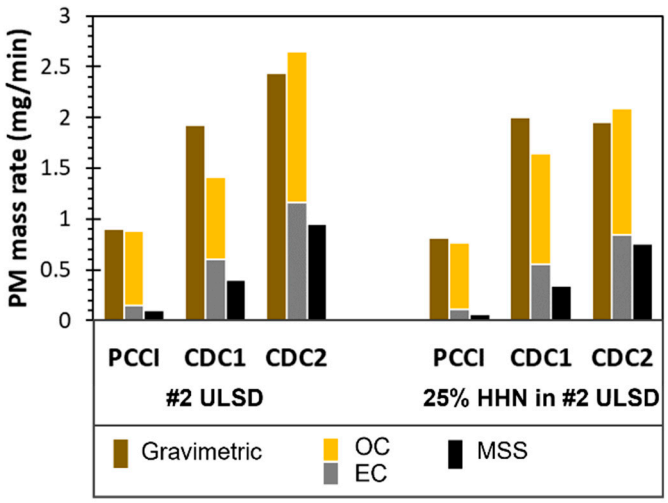

Figure 6. Comparison of PM emission results from gravimetric, EC/OC, and MSS in different engine modes with #2 ULSD and HHN blended fuel.

The high equivalence ratio of the LTC strategy can reduce the local rich combustion zones where PM is mainly formed, resulting in the PM emissions reduction seen in the PCCI mode. The reduction in PM mass in the PCCI mode suggested that a multimode approach that employs the PCCI over CDC1 mode at low loads would be beneficial for reducing PM emissions. While PCCI lowered the soot (EC PM) emission, it had little impact on the OC PM, which prevented a total suppression of the PM emissions. The lower equivalence ratio at the higher load condition, CDC2, created more fuel-rich zones, contributing to the higher PM emissions compared to CDC1.

It has been confirmed that biodiesel reduces soot PM formation and it has been suggested that both the promotion of cleaner combustion, associated with the higher oxygen content, and a reduction in fuel aromatics, which are known soot producers, contribute to the lower soot emissions from oxygenated biofuels [18]. The PM emissions, shown in Figure 6, support this with a noticeable reduction in both the EC and OC PM at the high-load condition, CDC2, when using 25%HHN blend fuel, while demonstrating insignificant changes at low load in both PCCI and CDC1.

Figures 7 and 8 describe total particle numbers (PNs) and the size distributions of particle emissions measured with the EEPS. Particulates from the engine exhaust went through a double-diluter conditioning system that included a thermal denuder temperature set at 150 °C or 350 °C before the measurements and are compared in Figure 7. It is not surprising that the total PN measured was lower at 350 °C for all conditions. There was no significant difference in the total PN emissions between the two low-load modes at 350 °C, whereas an increase was observed at the high-load condition, CDC2. The size distribution in Figure 8 indicates that the PCCI mode resulted in a significant drop in bigger-sized particles (≥50 nm) for both fuels compared to CDC1. Size distributions at 350 °C in both low- and high-load CDC modes were similar regardless of the fuel. However, bimodal size distributions were observed at 150 °C in CDC1 but not CDC2 for both fuels because of the small nuclei size of PN emissions. Using 25% HHN fuel always reduced the total PN emissions slightly but did not make a significant size distribution difference.

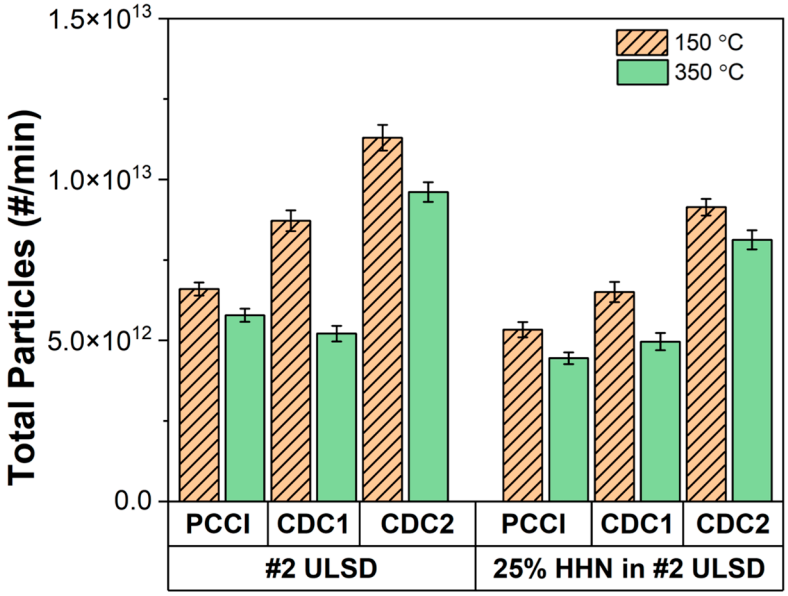

Figure 7. PN emissions measured by EEPS at low load (PCCI and CDC1) and high load (CDC2) for two fuels (#2 ULSD and 25% HHN blend). The PN rate for each mode/fuel combination was measured at thermal denuder temperatures of 150 °C and 350 °C.

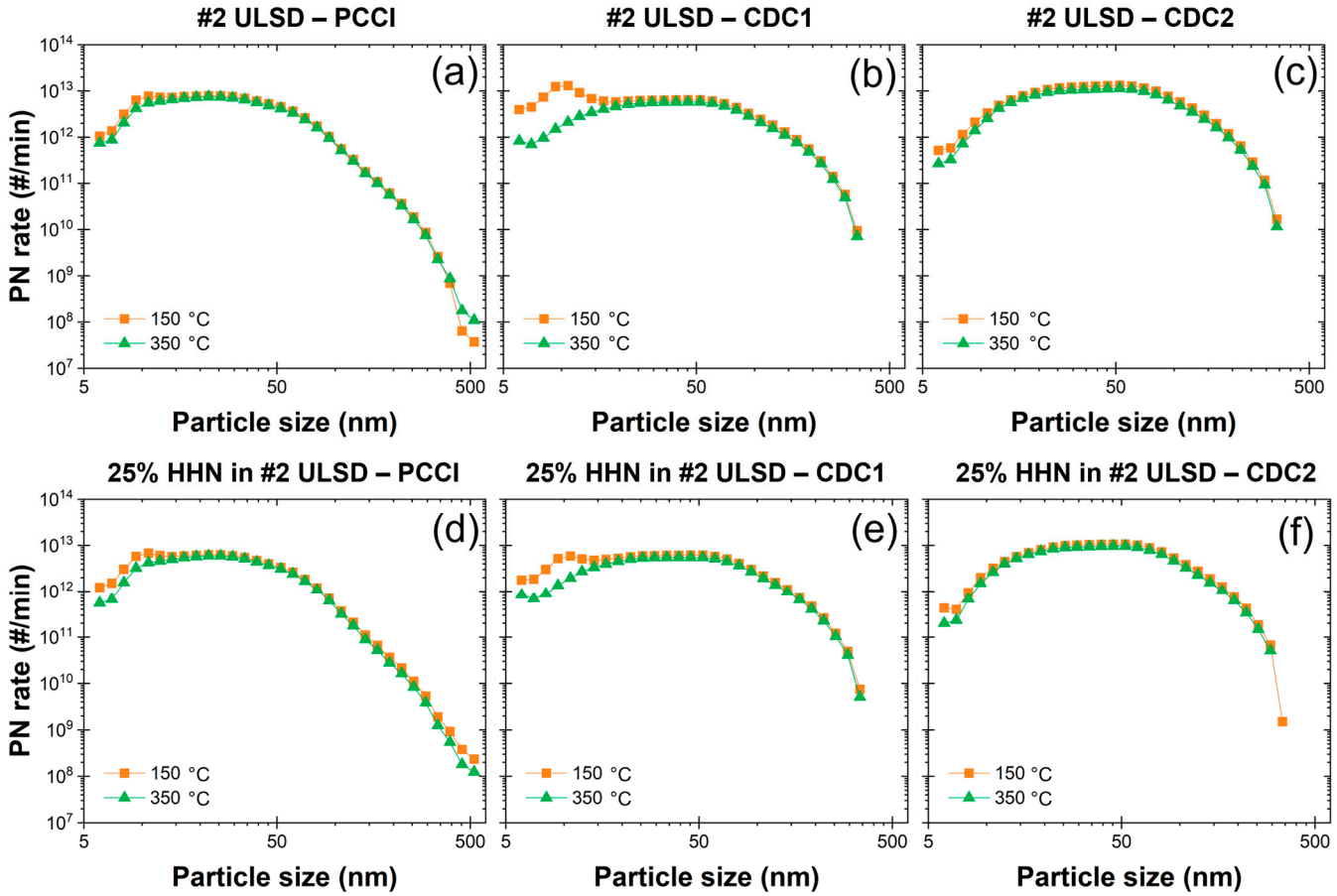

Figure 8. PN size distributions for (**a**) PCCI mode using #2 ULSD, (**b**) CDC1 mode using #2 ULSD, (**c**) CDC2 mode using #2 ULSD, (**d**) PCCI mode using HHN blend fuel, (**e**) CDC1 mode using HHN blend fuel, (**f**) CDC2 mode using HHN blend fuel. In all conditions, particulates are treated at two different temperatures, 150 °C and 350 °C, in a thermal denuder.

4. Discussion

4.1. Integrative THC Emissions Results

The HC mass rate differences were significant between the combined HCs (from FTIR, FTIR/DNPH, and canisters) and FID results in Figure 9. Based on the unquantified but identifiable species in the canister samples, the differences can be attributed to small semi-volatile species between the carbon numbers of C10 and C14. Regardless of these differences, PCCI reduced total HCs, and all three types of volatile paraffins contributed significantly to the reduction along with the larger, semi-volatile HCs. The FTIR speciation showed an increase in C1–C4 HCs in the PCCI mode. Not surprisingly, the increase in load from CDC1 to CDC2 mode resulted in more volatile aromatic species and more semi-volatile HCs.

The addition of 25% HHN to the fuel limited the volatile paraffin reduction in the PCCI mode but lowered the volatile aromatic emissions in CDC2, due to the dilution effect caused by the absence of aromatics in HHN.

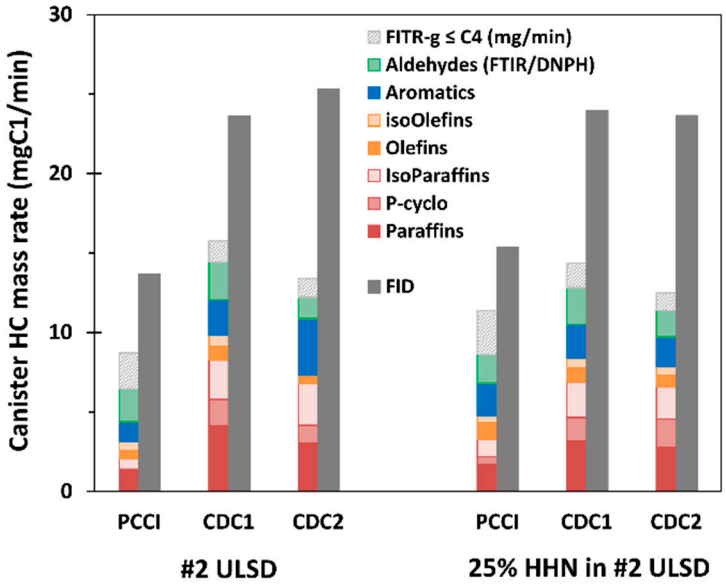

Figure 9. Grouped HC species combined analyzed from FTIR-g (≤C4, light grey), FTIR/DNPH (aldehydes, green), and canister (all the other HC species) measurements compared with FID results (dark grey).

4.2. Multimode Impact

LTC strategies like PCCI typically lower NOx and PM emissions due to lower combustion temperatures at the expense of increasing CO and THC emissions. In this study, PCCI mode increased CO emissions while reducing THC emissions. Under a low-load condition, the CO emissions from a conventional diesel tend to be low with sufficient excess oxygen and mixing time to fully oxidize CO after combustion with other products of fuel-rich combustion. However, low-load LTC conditions can result in post-combustion mixing that works towards a more fuel-lean condition, constraining CO oxidation in the post-combustion mixing [19], which may explain the higher CO but lower THCs in the PCCI mode of this study. Additionally, Han et al. [20] investigated HC and CO emissions from LTC modes using a blended fuel of gasoline and diesel and found that increased THC emissions were primarily affected by ignition delay, whereas increased CO emissions were closely related to the global equivalence ratio. The prolonged ignition delay was controlled either by expanding the gasoline ratio in the fuel or increasing the global equivalence ratio. They explained that extending the ignition delay can create a more overmixed region that can make fuel oxidation difficult and result in increasing HC emissions. Since ignition delay and the global equivalence ratio are related, the secondary impact of an HC emission increase was a global equivalence ratio; however, the effect of it is sensitive only when the global equivalence ratio is above 0.85. On the other hand, an increase in CO emissions occurred with the global equivalence ratio over the whole region they explored.

An increase in formaldehyde seen for PCCI compared to CDC1 (Figure 4) supports the lower temperature combustion expected for PCCI [21–27]. The expected temperature increase for CDC1 supports the potential that formaldehyde acted as an intermediate formed during the initial ignition process and was consumed in the later, high-temperature oxidation process. It aligns with the observation of higher formaldehyde formation in PCCI compared to CDC1, which coincided with a reduction in acetaldehyde and the other larger aldehydes. Despite the decreased total aldehyde emissions at the high-load condition, CDC2, both the C1 mass and fraction of the total aldehyde mass were found to be the lowest across the three conditions studied, regardless of the fuel.

4.3. Biofuel Impact

Multiple variables simultaneously impact engine emissions; however, there are general trends reported when using biodiesel. Lapuerta et al. [18] noted that 85% of publications

reported increased NOx emissions, 95% reported a decrease in PM and THCs, and 90% reported a decrease in CO when biodiesel was used. In this work, in the medium-duty multimode engine, NOx, CO, and THC emissions did not show significant differences, but decreases in PM and PN emissions were observed with 25% HHN fuel.

While changes in the total THC emissions were not observed when the 25% HHN fuel was used in this study, the fractions of specific species were influenced. Aromatic aldehydes are lower in the low-load modes, and volatile aromatic species are lower in the high-load modes with 25% HHN fuel. Mixed results have been reported for biodiesel's impact on aromatic emissions with more researchers observing decreased average aromatic and polyaromatic hydrocarbon emissions [28–34], while others report increases [35] or mixed results [32–34]. While it is expected that the lower fraction of aromatic compounds included in the 25% HHN fuel may promote the reduction of aromatic aldehydes in the low-load modes and volatile aromatics in the high-load mode, other complex combustion processes were likely involved in forming aromatics since this was not a general trend for all the modes. Considering aromatics are the main precursor to PM, the decrease in their presence within the fuel's composition would be expected to be a contributing factor to the observed reduction in PM and PN emissions with 25% HHN fuel.

5. Conclusions

Emissions from an MD multimode engine at two low-load modes (PCCI, CDC1) and one high-load mode (CDC2) were used to compare a multimode strategy (PCCI + CDC2) to a full CDC (CDC1 + CDC2). The impacts of biofuel blending on emissions in both the multimode and CDC combustion strategies were compared using #2 ULSD and a 25% HHN in #2 ULSD blended fuel. The PCCI mode used at low loads in the multimode strategy significantly decreased NOx, THC, and PM emissions but increased CO emissions, which can be easily oxidized by a standard oxidation catalyst.

The 25% HHN fuel lowered PM/PN emissions in all modes before thermal denuding (150 °C), providing a reduction in particulate emissions with both strategies. After thermal denuding (350 °C) removed semi-volatile condensate from the particulate, little impact was seen in either low-load mode. The multimode combustion strategy (PCCI + CDC2) offered the best overall reduction in emissions regardless of fuel. While the HHN blended fuel did not reduce emissions, it also did not cause any significant increase regardless of which strategy—traditional CDC or advanced multimode combustion—was used. This limited difference in HC compositions suggests that engines that run on this biofuel blend can use current aftertreatment catalysts for emissions control.

More subtle differences were seen in some emissions. Detailed THC species were analyzed and grouped by their functionality for a better understanding of emissions from different engine modes and fuel types.

- The decrease in THC in the PCCI mode was mainly associated with paraffins, but a slight increase in olefins, formaldehyde, and small C1–C4 HCs was also observed;
- The 25% HHN fuel had a minimal impact on the total HC emissions, but influenced the composition of the HCs emitted. It decreased aromatic aldehydes in the low-load modes and decreased volatile aromatics in the high-load mode.

The analysis of PM/PN emissions highlights the following:

- The PM reduction in PCCI mode was associated with particles $\geq$50nm;
- PN emissions after the 350 °C thermal denuding saw a small fuel effect at the high load (CDC2) with the use of 25% HHN blended fuel, causing a slight reduction as would be expected with blending reducing fuel aromatics;
- Both HHN blending and the multimode strategy reduced PN emissions without thermal denuding (150°C), with the biggest reduction coming from fuel blending in the full CDC strategy (CDC1 + CDC2);
- The lowest total PN emissions without thermal denuding (150 °C) were achieved with multimode (PCCI + CDC) combustion using the 25% HHN blended fuel.

Author Contributions: Y.P.: data curation, formal analysis, investigation, visualization, writing—original draft, writing—review and editing. M.M.-D.: conceptualization, data curation, formal analysis, investigation, funding acquisition, project administration, supervision, visualization, writing—original draft, writing—review and editing. S.S.S.: methodology, resources, supervision, writing—review and editing. S.P.H.: investigation, writing—review and editing. All authors have read and agreed to the published version of the manuscript.

Funding: This research was funded by UT-Battelle, LLC under Contract No. DE-AC05-00OR22725 with the U.S. Department of Energy.

Data Availability Statement: Data is included in the manuscript. Please contact corresponding author with further inquiries.

Acknowledgments: This research was conducted as part of the Co-Optimization of Fuels & Engines (Co-Optima) project sponsored by the U.S. Department of Energy (DOE) Office of Energy Efficiency and Renewable Energy (EERE) Bioenergy Technologies and Vehicle Technologies Offices. Co-Optima is a collaborative project of multiple national laboratories initiated to simultaneously accelerate the introduction of affordable, scalable, and sustainable biofuels and high-efficiency, low-emission vehicle engines. The authors would like to thank the U.S. DOE Co-Optima Programs Manager Kevin Stork and Gurpreet Singh for their support and guidance in this work. The authors would also like to acknowledge and thank Vlad Lobodin for running GC-MS and UV-Vis on the collected canister and DNPH samples.

Conflicts of Interest: The authors declare no conflict of interest.

Abbreviations

PCCI	premixed charge compression ignition
CDC	conventional diesel combustion
HC	hydrocarbon
PM	particulate matter
HHN	hexyl hexanoate
MDHD	medium-duty and heavy-duty
GHG	greenhouse gas
LTC	low-temperature combustion
wt%	weight percent
MSS	micro soot sensor
EEPS	engine exhaust particle sizer
MFC	mass flow controller
EC	elemental carbon
OC	organic carbon
THC	total hydrocarbon
FID	flame ionization detector
FTIR	Fourier-transform infrared spectrometer
g-FTIR	gasoline FTIR method
d-FTIR	diesel FTIR method
GC-MS	gas chromatograph—mass spectrometer
DNPH	2,4-dinitrophenylhydrazine
HPLC	high-performance liquid chromatograph
UV-Vis	ultraviolet–visible spectrometer
Qf	quartz filter
DGM	dry gas meter
PN	particle number
#/min	number per minute
CDC1	low-load CDC
CDC2	high-load CDC
ULSD	ultra-low sulfur diesel
NOx	nitrogen oxides
CO	carbon monoxide
CO_2	carbon dioxide

References

1. U.S. Department of State; U.S. Executive Office of the President. The Long-Term Strategy of the United States, Pathways to Net-Zero Greenhouse Gas Emissions by 2050. Washington D.C.; November 2021. Available online: https://unfccc.int/documents/308100 (accessed on 6 February 2023).
2. U.S. Department of Energy Alternative Fuels Data Center. *Average Annual Fuel Use by Vehicle Type (Last Updated February 2020)*. Available online: https://afdc.energy.gov/data/10308 (accessed on 6 February 2023).
3. Forrest, K.; Mac Kinnon, M.; Tarroja, B.; Samuelsen, S. Estimating the technical feasibility of fuel cell and battery electric vehicles for the medium and heavy duty sectors in California. *Appl. Energy* **2020**, *276*, 115439. [CrossRef]
4. Muratori, M.; Alexander, M.; Arent, D.; Bazilian, M.; Cazzola, P.; Dede, E.M.; Farrell, J.; Gearhart, C.; Greene, D.; Jenn, A.; et al. The rise of electric vehicles—2020 status and future expectations. *Prog. Energy* **2021**, *3*, 22002. [CrossRef]
5. Zhao, F.; Assanis, D.N.; Asmus, T.N.; Dec, J.E.; Eng, J.A.; Najt, P.M. *Homogeneous Charge Compression Ignition (HCCI) Engines: Key Research and Development Issues*; Society of Automotive Engineers: Warrendale, PA, USA, 2003.
6. Dec, J.E. Advanced compression-ignition engines—Understanding the in-cylinder processes. *Proc. Combust. Inst.* **2009**, *32*, 2727–2742. [CrossRef]
7. Krishnamoorthi, M.; Malayalamurthi, R.; He, Z.; Kandasamy, S. A review on low temperature combustion engines: Performance, combustion and emission characteristics. *Renew. Sustain. Energy Rev.* **2019**, *116*, 109404. [CrossRef]
8. Bobi, S.; Kashif, M.; Laoonual, Y. Combustion and emission control strategies for partially-premixed charge compression ignition engines: A review. *Fuel* **2021**, *310*, 122272. [CrossRef]
9. Fioroni, G.; Fouts, L.; Luecke, J.; Vardon, D.; Huq, N.; Christensen, E.; Huo, X.; Alleman, T.; McCormick, R.; Kass, M.; et al. Screening of Potential Biomass-Derived Streams as Fuel Blendstocks for Mixing Controlled Compression Ignition Combustion. *SAE Int. J. Adv. Curr. Prac. Mobil.* **2019**, *1*, 1117–1138. [CrossRef]
10. Burton, J.L.; Martin, J.A.; Fioroni, G.M.; Alleman, T.L.; Hays, C.K.; Ratcliff, M.A.; Thorson, M.R.; Schmidt, A.J.; Hallen, R.T.; Hart, T.R.; et al. *Fuel Property Effects of a Broad Range of Potential Biofuels on Mixing Control Compression Ignition Engine Performance and Emissions*; SAE Technical Paper 2021-01-0505; SAE: Warrendale, PA, USA, 2021. [CrossRef]
11. Sluder, C.S.; Curran, S.J. Diesel-Range Fuel Property Effects on Medium-Duty Advanced Compression Ignition for Low-Load NO_X Reduction. *SAE Int. J. Fuels Lubr.* **2022**, *16*, 57–74. [CrossRef]
12. Curran, S.; Szybist, J.; Kaul, B.; Easter, J.; Sluder, S. Fuel Stratification Effects on Gasoline Compression Ignition with a Regular-Grade Gasoline on a Single-Cylinder Medium-Duty Diesel Engine at Low Load. *SAE Int. J. Adv. Curr. Pract. Mobil.* **2021**, *4*, 488–501. [CrossRef]
13. Parks, J.E.; Storey, J.; Prikhodko, V.; Moses-DeBusk, M.; Lewis, S.A. *Filter-Based Control of Particulate Matter from a Lean Gasoline Direct Injection Engine*; SAE Technical Paper 2016-01-0937; SAE: Warrendale, PA, USA, 2016. [CrossRef]
14. Birch, M.E.; Cary, R.A. Elemental Carbon-Based Method for Monitoring Occupational Exposures to Particulate Diesel Exhaust. *Aerosol. Sci. Technol.* **1996**, *25*, 221–241. [CrossRef]
15. Gierczak, C.A.; Kralik, L.L.; Mauti, A.; Harwell, A.L.; Maricq, M.M. Measuring NMHC and NMOG emissions from motor vehicles via FTIR spectroscopy. *Atmos. Environ.* **2017**, *150*, 425–433. [CrossRef]
16. Park, Y.; Moses-DeBusk, M.; Powell, T.; Szybist, J.; Xiang, Z.; Zhu, J.; McEnally, C.S.; Pfefferle, L.D. Fuel property impacts on gaseous and PM emissions from a multi-mode single-cylinder engine. *Fuel* **2023**, *331*, 125641. [CrossRef]
17. Moses-DeBusk, M.; Storey, J.M.; Lwis Sr, S.A.; Connatser, R.M.; Mahurin, S.M.; Huff, S.; Thompson, C.V.; Park, Y. Detailed hydrocarbon speciation and particulate matter emissions during cold-start from turbocharged and naturally aspirated trucks. *Fuel* **2023**, *350*, 128804. [CrossRef]
18. Lapuerta, M.; Armas, O.; Fernández, J.R. Effect of biodiesel fuels on diesel engine emissions. *Prog. Energy Combust. Sci.* **2008**, *34*, 198–223. [CrossRef]
19. Musculus, M.P.; Miles, P.C.; Pickett, L.M. Conceptual models for partially premixed low-temperature diesel combustion. *Prog. Energy Combust. Sci.* **2013**, *39*, 246–283. [CrossRef]
20. Han, D.; Ickes, A.M.; Bohac, S.V.; Huang, Z.; Assanis, D.N. HC and CO emissions of premixed low-temperature combustion fueled by blends of diesel and gasoline. *Fuel* **2012**, *99*, 13–19. [CrossRef]
21. Kosaka, H.; Drewes, V.H.; Catalfamo, L.; Aradi, A.A.; Iida, N.; Kamimoto, T. *Two-Dimensional Imaging of Formaldehyde Formed during the Ignition Process of a Diesel Fuel Spray*; SAE Technical Paper 2000-01-0236; SAE: Warrendale, PA, USA, 2000. [CrossRef]
22. Collin, R.; Nygren, J.; Richter, M.; Aldén, M.; Hildingsson, L.; Johansson, B. *Simultaneous OH- and Formaldehyde-LIF Measurements in an HCCI Engine*; SAE Technical Paper 2003-01-3218; SAE: Warrendale, PA, USA, 2003. [CrossRef]
23. Hildingsson, L.; Persson, H.; Johansson, B.; Collin, R.; Nygren, J.; Richter, M.; Aldén, M.; Hasegawa, R.; Yanagihara, H. *Optical Diagnostics of HCCI and Low-Temperature Diesel Using Simultaneous 2-D PLIF of OH and Formaldehyde*; SAE Technical Paper 2004-01-2949; SAE: Warrendale, PA, USA, 2004. [CrossRef]
24. Kashdan, J.T.; Papagni, J.-F. *LIF Imaging of Auto-Ignition and Combustion in a Direct Injection Diesel-Fuelled HCCI Engine*; SAE Technical Paper 2005-01-3739; SAE: Warrendale, PA, USA, 2005. [CrossRef]
25. Parks, J.E.; Prikhodko, V.; Storey, J.M.; Barone, T.L.; Lewis, S.A.; Kass, M.D.; Huff, S.P. Emissions from premixed charge compression ignition (PCCI) combustion and affect on emission control devices. *Catal. Today* **2010**, *151*, 278–284. [CrossRef]
26. Prikhodko, V.Y.; Curran, S.J.; Barone, T.L.; Lewis, S.A.; Storey, J.M.; Cho, K.; Wagner, R.M.; Parks, J.E. Emission Characteristics of a Diesel Engine Operating with In-Cylinder Gasoline and Diesel Fuel Blending. *SAE Int. J. Fuels Lubr.* **2010**, *3*, 946–955. [CrossRef]

27. Singh, A.P.; Agarwal, A.K. Performance and emission characteristics of conventional diesel combustion/partially premixed charge compression ignition combustion mode switching of biodiesel-fueled engine. *Int. J. Engine Res.* **2019**, *22*, 540–553. [CrossRef]
28. Sharp, C.A.; Howell, S.A.; Jobe, J. *The Effect of Biodiesel Fuels on Transient Emissions from Modern Diesel Engines, Part II Unregulated Emissions and Chemical Characterization*; SAE Technical Paper 2000-01-1968; SAE: Warrendale, PA, USA, 2000. [CrossRef]
29. Durbin, T.D.; Collins, J.R.; Norbeck, J.M.; Smith, M.R. Effects of Biodiesel, Biodiesel Blends, and a Synthetic Diesel on Emissions from Light Heavy-Duty Diesel Vehicles. *Environ. Sci. Technol.* **1999**, *34*, 349–355. [CrossRef]
30. Turrio-Baldassarri, L.; Battistelli, C.L.; Conti, L.; Crebelli, R.; De Berardis, B.; Iamiceli, A.L.; Gambino, M.; Iannaccone, S. Emission comparison of urban bus engine fueled with diesel oil and 'biodiesel' blend. *Sci. Total. Environ.* **2004**, *327*, 147–162. [CrossRef]
31. Lin, Y.-C.; Lee, W.-J.; Hou, H.-C. PAH emissions and energy efficiency of palm-biodiesel blends fueled on diesel generator. *Atmos. Environ.* **2006**, *40*, 3930–3940. [CrossRef]
32. Corrêa, S.M.; Arbilla, G. Aromatic hydrocarbons emissions in diesel and biodiesel exhaust. *Atmos. Environ.* **2006**, *40*, 6821–6826. [CrossRef]
33. Yang, H.-H.; Chien, S.-M.; Lo, M.-Y.; Lan, J.C.-W.; Lu, W.-C.; Ku, Y.-Y. Effects of biodiesel on emissions of regulated air pollutants and polycyclic aromatic hydrocarbons under engine durability testing. *Atmos. Environ.* **2007**, *41*, 7232–7240. [CrossRef]
34. He, C.; Ge, Y.; Tan, J.; You, K.; Han, X.; Wang, J. Characteristics of polycyclic aromatic hydrocarbons emissions of diesel engine fueled with biodiesel and diesel. *Fuel* **2010**, *89*, 2040–2046. [CrossRef]
35. Pedersen, J.R.; Ingemarsson, A.; Olsson, J.O. Oxidation of Rapeseed Oil, Rapeseed Methyl Ester (Rme) and Diesel Fuel Studied with Gc/Ms. *Chemosphere* **1999**, *38*, 2467–2474. [CrossRef]